Deformed Hexagonal Patterns in a Weakly Anisotropic System

Rainer Schmitz, Walter Zimmermann

Deformed Hexagonal Patterns in a Weakly Anisotropic System

Rainer Schmitz (1) and Walter Zimmermann (1,2,*)

(1) Institut für Festkörperforschung, Forschungszentrum Jülich, 52425 Jülich, Germany
(2) FORUM Modellierung, Forschungszentrum Jülich, 52425 Jülich, Germany

(Received 16 July 1996, revised 21 November 1996, accepted 8 January 1997)

PACS.47.20.-k – Hydrodynamic stability
PACS.03.40.Gc – Fluid dynamics: general mathematical aspects

Abstract. — For a two–dimensional model of pattern formation the interplay between a broken up down symmetry and a weakly broken rotational symmetry is investigated. Both symmetries may be broken, for instance, in chemical reactions with an applied electric field or in thermal convection of planarly aligned nematic liquid crystals. In a system with rotational symmetry and a broken up down symmetry hexagonal patterns are favored in a certain parameter range. With increasing values for the anisotropies, by keeping the up down symmetry broken, hexagons may be deformed to centered rectangular patterns. Hence, breaking both symmetries is an alternative mechanism leading to rectangular patterns. Finally, at larger values of the anisotropies a bifurcation to stripes takes place.

1. Introduction

Competition between different patterns occurs in many systems far from thermal equilibrium [1, 2]. Two examples are chemical reactions [3] or Rayleigh–Bénard convection [4, 5] where transitions between striped patterns and hexagons have been observed. Both are experimentally well–controlled systems and the understanding of the hexagon–stripe transition has reached a quantitative level [3, 6–8]. Besides these systems, which are isotropic in a plane, there is another class of two–dimensional extended systems with a broken rotational invariance. Thermal convection and electroconvection in planarly aligned nematic liquid crystals have an intrinsic anisotropy and belong to this class. During the recent decade both systems have been extensively investigated [9, 10].

It is an interesting and open question which kind of effects may be expected if the up–down and the rotational symmetry are broken simultaneously. Here we investigate for a model system this question by varying the parameters of the anisotropy and the coefficient ruling the up–down symmetry breaking. For a broken up–down symmetry it will be shown how increasing values of the anisotropy parameters deform hexagonal patterns into rectangular like patterns. Both symmetries might be broken in chemical reactions where hexagons occur and where the isotropy is broken simultaneously by an external ac electric field [11–13]. Another example is thermal convection in planarly aligned nematic liquid crystals. It is an anisotropic pattern forming system (see *e.g.* [10.14] and Refs. therein) and the up- down symmetry might

(*) Author for correspondence (e-mail:W.Zimmermann@kfa-juelich.de)

be broken in the so–called non–Boussinesq regime or by a pretilt–angle between the nematic orientational order and the confining boundary.

2. Model Equation

With the Swift–Hohenberg equation a model is known that describes periodic patterns in two–dimensional isotropic systems and essential features of thermal convection near onset [15]. This model is invariant with respect to rotations and changes of the sign of the field. Later on, this model has been extended by adding a quadratic nonlinearity which removes the $\pm$ symmetry [16] and which mimics in thermal convection the so–called non–Boussinesq effects [4]. By another extension the rotational invariance is broken and describes some features of pattern formation in anisotropic systems, such as convection in planarly aligned nematic liquid crystals [17]. The interplay between a special form of the anisotropy and the broken up–down symmetry has been considered, too [18,19]. Here we generalize these models by combining the general anisotropic formulation with a quadratic nonlinearity:

$$\partial_t u = \left[\varepsilon - \left(q_0^2 + \nabla^2\right)^2\right]u + bu^2 - u^3 + 2\left(\alpha_1 \partial_x^2 - \alpha_2 \partial_x^2 \partial_y^2\right)u. \tag{1}$$

The rotational symmetry is broken for $\alpha_i \neq 0$ and the up down symmetry, $u \to -u$, is broken for a non–vanishing coefficient in front of the quadratic term, $b \neq 0$. One might imagine additional gradients in the nonlinearities, such as in the Kuramoto–Sivashinsky equation [20,21], and such terms might be anisotropic too. Since we are only interested in a few qualitative aspects of the interplay between both broken symmetries, we do not take into account such additional anisotropic effects.

3. Threshold

The stability of the basic state, $u \equiv 0$, is investigated with the ansatz $u = F \exp[\lambda t + i(qx + py)]$ ($F \ll \varepsilon$). Above the neutral curve, $\varepsilon_0(q,p)$, the growth rate $\mathrm{Re}(\lambda)$ becomes positive,

$$\varepsilon_0(q,p) = (q_0^2 - q^2 - p^2)^2 + 2\alpha_1 q^2 + 2\alpha_2 q^2 p^2\,, \tag{2}$$

and the basic state becomes unstable. This neutral surface $\varepsilon_0(q,p)$ has extrema at $q_c^2 = q_0^2 - \alpha_1$, $p_c = 0$ with $\varepsilon_c(q_c,\ p_c = 0) = 2\alpha_1 q_0^2 - \alpha_1^2$ and at $q_c = 0$, $p_c = q_0$ with $\varepsilon_c(q_c = 0,\ p_c = 1) = 0$. For $\alpha_2 = 0$ and $1 > \alpha_1 > 0$ ($\alpha_1 < 0$) the first extremum corresponds to a saddle (global minimum) and the second one to a global minimum (saddle) of $\varepsilon_0(q,p)$. If $\alpha_2 > 0$ the saddle changes to a local minimum. For $-1 < \alpha_2 < 0$ and $\alpha_1 > \alpha_2/(1+\alpha_2)$ the global minimum of the neutral surface ε_0 is at

$$q_c^2 = -\frac{\alpha_1 + \alpha_2 q_0^2}{1 - (1+\alpha_2)^2}\,, \qquad p_c^2 = \frac{\alpha_1(1+\alpha_2) - q_0^2 \alpha_2}{1 - (1+\alpha_2)^2}\,, \tag{3}$$

and one has the so–called oblique roll instability [9, 10, 17, 22]. The previous two extrema at $q_c = 0$, $p_c = q_0$ and $q_c = q_0^2 - \alpha_1$, $p_c = 0$ become saddles.

4. Weakly Nonlinear Behavior

The behavior of periodic solutions with constant complex amplitudes, A_i, may be investigated near threshold with a three–mode ansatz of the following form [3, 4, 7]

$$u(x,y,t) = A_1\, \mathrm{e}^{iqx} + A_2\, \mathrm{e}^{i\,\mathbf{q}_2 \mathbf{r}} + A_3 \mathrm{e}^{i\,\mathbf{q}_3 \mathbf{r}} + \mathrm{cc.}\,, \tag{4}$$

(cc. = conj. complex and $\mathbf{r} = (x, y)$). The wave vectors $\mathbf{q}_{2,3}$ are defined as

$$\mathbf{q}_{2,3} = \frac{q}{2}\Big(-1, \pm\sqrt{3}(1+P)\Big) . \tag{5}$$

For $P \neq 0$ the solution (4) corresponds to a slightly deformed hexagonal pattern [3]. If only one of the three amplitudes A_i is excited, equation (1) describes a stripe pattern.

With the scaling of the amplitudes $A_i \propto \varepsilon^{1/2}$ and of the nonlinear coefficient $b \propto \varepsilon^{1/2}$ the following set of coupled equations can be derived from equations (1) [4, 7]

$$\tau_0 \partial_t A_1 = \eta_a A_1 + 2bA_2^* A_3^* - f(A_1)A_1 , \tag{6a}$$
$$\tau_0 \partial_t A_2 = \eta_b A_2 + 2bA_1^* A_3^* - f(A_2)A_2 , \tag{6b}$$
$$\tau_0 \partial_t A_3 = \eta_b A_3 + 2bA_1^* A_2^* - f(A_3)A_3 , \tag{6c}$$

with the abbreviations

$$f(A_i) = \gamma \mid A_i \mid^2 + \rho \sum_{j\neq i} \mid A_j \mid^2 , \tag{7a}$$
$$\gamma = 3 , \qquad \rho = 6 ,$$
$$\eta_a = \varepsilon - \left(q_0^2 - q^2\right)^2 - 2\alpha_1 q^2 , \tag{7b}$$
$$\eta_b = \varepsilon - \left(q_0^2 - \frac{q^2}{4}(1 + 3(1+P)^2)\right)^2 - \alpha_1 q^2/2 - 3\frac{\alpha_2 q^4}{8}(1+P)^2 \tag{7c}$$

Equations (6) can be derived from a potential

$$\partial_t A_i = -\frac{1}{\tau_0}\frac{\delta \mathcal{F}}{\delta A_i^*} , \tag{8}$$

with

$$\begin{aligned} \mathcal{F}_h = & \frac{1}{2}\int \mathrm{d}x\,\mathrm{d}y \Big[\sum_{i=1,2,3} \frac{\gamma}{2} \mid A_i \mid^4 - \eta_a \mid A_1 \mid^2 \\ - & \eta_b \Big(\mid A_2 \mid^2 + \mid A_3 \mid^2 \Big) \\ - & 2b\Big(A_1 A_2 A_3 + A_1^* A_2^* A_3^*\Big) \\ + & \rho\Big(\mid A_1 \mid^2 (\mid A_2 \mid^2 + \mid A_3 \mid^2) + \mid A_2 \mid^2 \mid A_3 \mid^2 \Big)\Big] . \end{aligned} \tag{9a}$$

For a hexagonal pattern the amplitudes are all equal, $A_i = A$, and A takes for $\mid \mathbf{q}_i \mid = q_0$ the form

$$A = \left[b \pm \left(b^2 + \varepsilon(\gamma + 2\rho)\right)^{1/2}\right] \Big/ \Big(\gamma + 2\rho\Big) . \tag{10}$$

The potential (9) per unit area, $\overline{\mathcal{F}}$, reduces for hexagons to

$$\overline{\mathcal{F}} = \frac{1}{4}\left[\frac{3}{2}(\gamma + 2\rho)A^4 - 3\eta A^2 - 4bA^3\right] . \tag{11}$$

If $\eta_a \neq \eta_b$ then equations (6) still have constant amplitude solutions with unequal amplitudes, $A_1 \neq A_2 = A_3$. Those resemble for $A_1 \ll A_2, A_3$ a rectangular pattern (*cf.* Fig. 4b) and for $A_1 > A_2, A_3$ the patterns resembles a slightly deformed hexagon (*cf.* Fig. 4c).

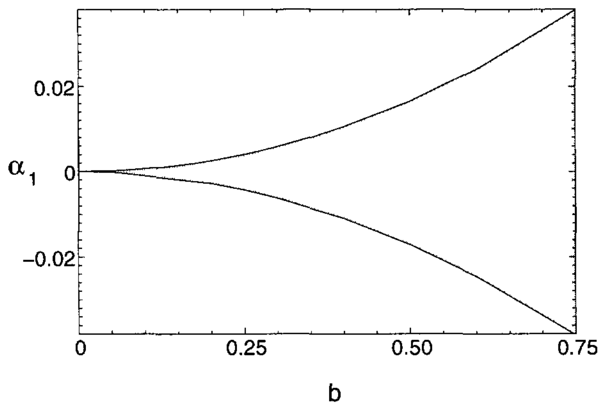

Fig. 1. — Along the solid line the functional $\mathcal{F}$ for the three–mode solutions of equations (6) vanishes at threshold $\varepsilon_c = 0$ (*cf.* Eq. (9)). For values of α_1 and b from the shaded region there is a finite range for ε where the three–mode solution is favored. In the unshaded range single mode solutions are always preferred beyond threshold ($\alpha_2 = 0$).

5. Results

Hexagonal patterns bifurcate subcritical [4], as can be seen from equation (10). Thus the amplitude A is already finite at threshold, $\varepsilon_c = 0$. The functional $\mathcal{F}$ with A from equation (10) is negative at threshold, ε_c, and thus lower than $\mathcal{F}$ for the basic state, $A \equiv 0$. For $b^2 \propto \varepsilon^{1/2} < 28/39$ stripes bifurcate supercritically, what we always assume throughout of this work. Hence the functional $\mathcal{F}$ for stripes vanishes at threshold and hexagonal patterns (*cf.* Fig. 4) are preferred in a finite range beyond threshold. For increasing values of ε the functional $\mathcal{F}$ for stripes decreases faster than for hexagons and above a critical value for the control parameter ε_b ($\varepsilon_b > \varepsilon_c$) single mode solutions have the lowest value for the functional and are preferred [4, 7].

In anisotropic systems, such as in electroconvection in planarly aligned nematic liquid crystals [9, 10], hexagonal patterns are not met. According to this observation we expect that for large values of the anisotropic coefficients α_i hexagons are suppressed in our model.

At finite values for the anisotropic coefficients α_i the bifurcation point ε_b will be reduced and the linear coefficients η_a and η_b in equations (6) as well as the constant solutions are unequal, $A_1 \neq A_2 = A_3$.

If the functional (9) vanishes at threshold for three–mode solutions and for a certain subset of parameters, (α_1, α_2, b), then one has $\varepsilon_b = 0$ and stripes are preferred beyond threshold. Accordingly the condition $\mathcal{F}(\varepsilon = \varepsilon_c) = 0$ for the three–mode ansatz or $\varepsilon_b = 0$ provides a curve in parameter space (b, α_1, α_2) which separates the range with preference of stripes from that where hexagons are favored at least in a finite range of ε.

If $\alpha_2 = 0$ is kept fixed then from the condition $\mathcal{F} = 0$ for the three–mode ansatz the critical values α_{1c}, at which the transition between three–mode solutions and stripes takes place, can be calculated as function of the nonlinear coefficient b. The two curves $\alpha_{1c}(b)$ are drawn in Figure 1 and for parameters from the shaded region between both curves the three–mode solutions are favored in a finite range of ε. Keeping $b = 0.5$ fixed, then with the same condition, $\mathcal{F} = 0$, the values for the parameters α_1, α_2 can be calculated where the three–mode solutions exist in a finite ε–range too, *cf.* shaded region in Figure 2. Beyond the shaded range in Figure 2 single mode solutions of equation (6) are always preferred. During the calculations

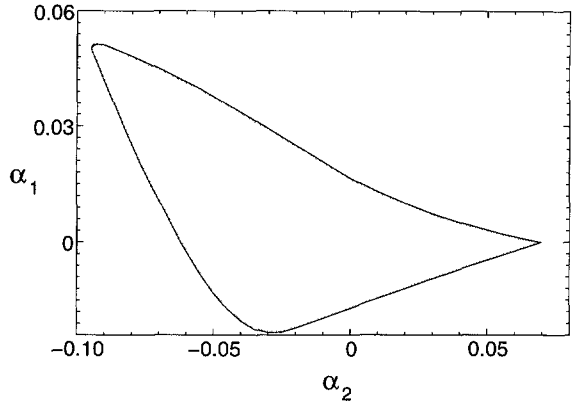

Fig. 2. — For parameters α_i from the shaded area there is a finite range for the control parameter ε where the functional (9) takes its absolute minimum for a three-mode solution of equations (6). $b = 0.5$ is fixed.

for Figures 1–3 the functional $\mathcal{F}$ has been always minimized with respect to the wave numbers q and P, however, minima of $\mathcal{F}$ stay always rather close to $q = q_0$ and $P = 0$, respectively.

Depending on the parameters, α_1, α_2 and b, the three-mode solutions of equations (6), $A_i \neq 0$, correspond to hexagons for $\alpha_1 = \alpha_2 = 0$ (*cf.* Fig. 4a), to deformed hexagons for $A_1 > A_2 = A_3$ (*cf.* Fig. 4c) or to a centered rectangular pattern for $A_1 \ll A_2 = A_3$ (*cf.* Fig. 4b). In Figures 4a–c the control parameter $\varepsilon = 0$ was fixed and for Figure 4d $\varepsilon = 0.1$ was chosen. At the values $\varepsilon = 0.1$, $b = 0.5$ and $\alpha_2 = 0$ one obtains for $\alpha_1 = 0.1$ stripes parallel to the x–axis (horizontal) and for $\alpha_1 = -0.1$ stripes parallel to y–axis, as indicated by formula (3). In Figure 4d α_1 is continuously ramped along the x–axis from $\alpha_1 = 0.1$ at the left to $\alpha_1 = 0.0$ in the middle and to $\alpha_1 = 0.1$ at the right. According to this ramp hexagons and stripes coexist, similar as in experiments [23] and for a previous model [24, 25]. The bending of the stripes near the transition to hexagons in Figure 4d is a further remarkable feature.

Figure 3 shows for a three–mode solution the variation of the ratio $A_1/A_{2,3}$ as function of α_1 and for a fixed value $b = 0.5$. The solid line in Figure 3 corresponds to $\alpha_2 = 0$ and the dashed line is calculated for $\alpha_2 = -2\alpha_1$. These two curves give an impression over which range the ratio $A_1/A_{2,3}$ is varying for parameters from the shaded region of Figures 1 and 2.

Rectangular patterns occur, for example, in thermal convection in planarly aligned nematic liquid crystals [14, 26] or under spatial forcing [27]. A rectangular pattern can be described by a superposition of two–straight rolls enclosing a finite angle in between. The amplitudes of both modes obey two coupled equations, $\partial_t A_{1,2} = [\varepsilon - \gamma \mid A_{1,2} \mid^2 - \rho \mid A_{2,1} \mid^2] A_{1,2}$, as can be obtained from equations (6) with $A_3 = 0$ and $b = 0$. The coexisting solution of these two coupled equations, $A_1 = A_2 \neq 0$, requires for stability the condition $\rho < \gamma$.

Calculating for specific systems the amplitude equations for two interacting modes, then one obtains quite often for the nonlinear coefficients the inequality $\rho > \gamma$. For this inequality the two mode solutions are unstable and only one mode survives. Figure 4b shows a solution for the parameters $b = 0.5$, $\alpha_1 = 0.05$ and $\alpha_2 = -0.094$, which resembles a centered rectangular pattern similar as one obtains for a superposition of two periodic solutions, *e.g.* $A_2 = A_3$, $A_1 = 0$. However, the solution given in Figure 4b is a three–mode solution (*cf.* Eq. (4)) with large amplitudes A_2 and A_3 and a small amplitude A_1 with a ratio of about $A_1/A_2 = 0.073$. In addition we have for our model still $\rho > \gamma$. In spite of having $\rho > \gamma$, a broken up–down symmetry, $b \neq 0$, can still favor rectangular like pattern by exciting a third mode, A_1. In this

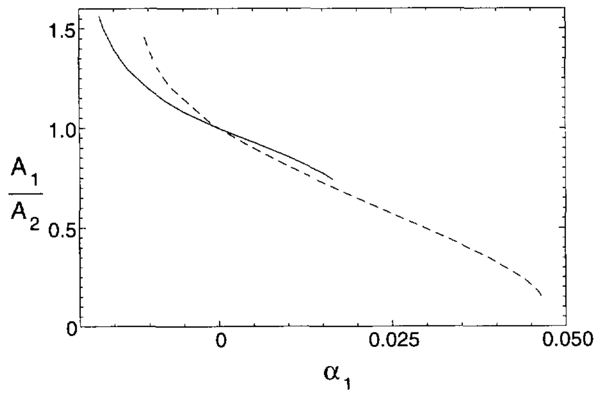

Fig. 3. — For three-mode solutions (4) the ratio $\frac{A_1}{A_{2\ 3}}$ between the amplitudes A_1 and $A_{2,3}$ is shown as function of the anisotropies $\alpha_{1,2}$ and for $b = 0.5$. Along the solid curve α_1 is varying and $\alpha_2 = 0$ is fixed and the dashed line describes the ratio, $\frac{A_1}{A_{2\ 3}}$, along the curve $\alpha_2 = -2\alpha_1$.

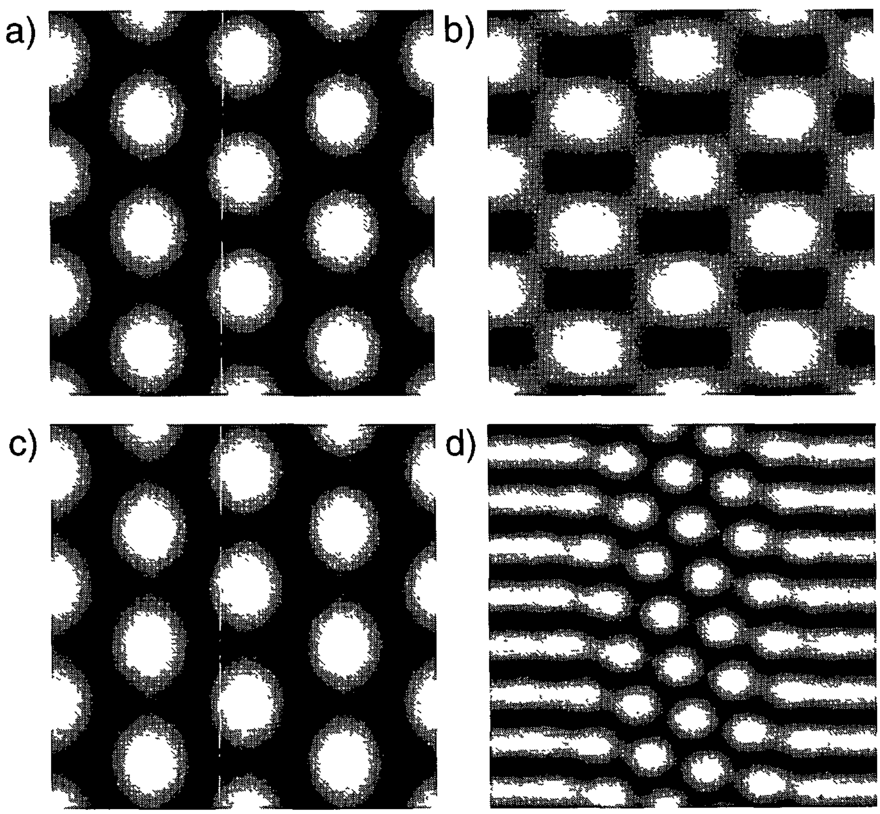

Fig. 4. — The spatial structure of patterns described by three-mode solutions of equations (6) for a fixed value $b = 0.5$ and different anisotropies: a) $\alpha_1 = \alpha_2 = 0$, b) $\alpha_1 = 0.05$ and $\alpha_2 = -0.094$, c) $\alpha_1 = -0.022$ and $\alpha_2 = -0.02$. Part d) shows a structure with α_1 varying along the horizontal direction (similar as in Ref. [13]). In a)–c) $\varepsilon = 0$ was fixed in d) $\varepsilon = 0.1$ has been chosen.

case the small amplitude A_1 serves for a coupling of the two strong modes $A_2 = A_3$ to form a rectangular pattern. This mechanism for stable rectangular patterns is rather different from the common case, however, it might be not easy to discriminate between both mechanisms in experiments.

It is therefore an interesting question whether experimental observations of rectangular pattern correspond always to a bimodal structure or to a three-mode solution with a small third mode (requiring a broken up-down symmetry) as described here. While the patterns look for both cases very similar, the mechanism leading to the coupling of two modes is rather different. This alternative mechanism leading to rectangular pattern is especially interesting in cases when centered rectangular patterns are observed in experiments such as in thermal convection in planarly aligned nematic liquid crystals, however, when *ab-initio* calculations for the same system show the opposite, namely, unstable rectangular pattern.

References

[1] Spatio-Temporal Patterns in Nonequilibrium Complex Systems, Vol. XXI of Santa Fe Institute Studies in the Sciences of Complexity, P. Cladis and P. Palffy-Muhoray, Eds. (Addision-Wesley, New York, 1995).
[2] Cross M.C. and Hohenberg P.C., *Rev. Mod. Phys.* **65** (1993) 851.
[3] Gunaratne G., Quyang Q. and Swinney H.L., *Phys. Rev. E* **50** (1994) 2802.
[4] Busse F.H., *J. Fluid Mech.* **30** (1967) 625.
[5] Busse F.H., in Hydrodynamic Instabilities and the Transition to Turbulence Vol. 45 of "Topic in Applied Physics", H.L. Swinney and J.P. Gollub, Eds. (Springer, New York, 1981).
[6] Heutmaker M.S. and Gollub J.P., *Phys. Rev. A* **35** (1987) 242.
[7] Ciliberto S., Pampaloni E. and Perez-Garcia C., *Phys. Rev. Lett.* **61** (1988) 1198.
[8] Bodenschatz E., DeBruyn J.R., Ahlers G. and Cannell D.S., *Phys. Rev. Lett.* **67** (1991) 3078.
[9] Zimmermann W., *Mat. Res. Bulletin* **16** (1991) 46.
[10] Kramer L. and Pesch W., *Ann. Rev. Fluid Mech.* **27** (1995) 515.
[11] Schmidt S.L. and Ortoleva P., *J. Chem. Phys.* **74** (1981) 4488.
[12] Sevcikova H. and Mareck M., *Physica D* **13** (1984) 379.
[13] Münster A.F., Hasal P., Snita D. and Marek M., *Phys. Rev. E* **50** (1994) 546.
[14] Berge L.I., Ahlers G. and Cannell D.S., *Phys. Rev. E* **48** (1993) 3236.
[15] Swift J.B. and Hohenberg P.C., *Phys. Rev. A* **15** (1977) 315.
[16] Bestehorn M. and Haken H., *Phys. Lett. A* **99** (1983) 265.
[17] Pesch W. and Kramer L., *Z. Physik B* **63** (1986) 121.
[18] Walgraef D. and Schiller C., *Physcia D* **27** (1987) 423.
[19] Guazelli E., Dewel G., Brockmans P. and Walgraef D., *Physcia D* **35** (1989) 220.
[20] Kuramoto Y., Chemical Oscillations, Waves, and Turbulence (Springer, Berlin, 1984).
[21] Sivashinsky G.I., *Ann. Rev. Fluid Mech.* **15** (1983) 1983.
[22] Zimmermann W. and Kramer L., *Phys. Rev. Lett.* **55** (1985) 402.
[23] Watzl M. and Münster A.F., *Chem. Phys. Lett.* **242** (1995) 273.
[24] Boissonade J., *J. Phys. France* **49** (1988) 541.
[25] Borckmans P., Wit A.D. and Dewel G., *Physica A* **188** (1992) 137.
[26] Ahlers G., in Pattern Formation in Liquid Crystals, A. Buka and L. Kramer, Eds. (Springer, Berlin, 1996).
[27] Zimmermann W., *et al.*, *Europhys. Lett.* **24** (1993) 217.